# Rotovibrational collision-induced absorption by nonpolar gases and mixtures ($H_2$-He pairs): Symmetry of line profiles

Massimo Moraldi
*Dipartimento di Fisica dell'Università di Firenze, I-50125 Firenze, Italy*

Aleksandra Borysow
*Joint Institute for Laboratory Astrophysics, University of Colorado, Boulder, Colorado 80309-0440*

Lothar Frommhold
*Department of Physics, University of Texas at Austin, Austin, Texas 78712-1081*
(Received 24 February 1988)

Intermolecular-interaction potentials depend on the vibrational coordinates of the molecules involved. We study the effect of this $v$ dependence (as we will call it for brevity) on the symmetry of line shapes of rotovibrational collision-induced-absorption (RVCIA) spectra of collisional complexes such as $H_2$-He or $H_2$-$H_2$. If the $v$ dependence is ignored, individual line shapes $\Gamma(\omega)$ of CIA spectra satisfy the widely used "detailed balance" relationship $\Gamma(-\omega)=e^{-\hbar\omega/kT}\Gamma(\omega)$, where $\omega$ designates the frequency shift relative to the molecular transition frequency, and $T$ the temperature. However, if one accounts for the $v$ dependence, the symmetry of a computed profile is modified significantly, the more so the higher the temperature and the higher the vibrational overtones one considers. These differing symmetries are described in quantitative terms that are of interest in modeling or analyzing RVCIA spectra. This paper may be considered the second, concluding part of our theoretical study of the influence of the $v$ dependence on RVCIA spectra; the previous part [Phys. Rev. A **36**, 4700 (1987)] deals with the influence of the $v$ dependence on the integrated intensities (spectral moments) of RVCIA spectra.

## I. INTRODUCTION

Nonpolar, tenuous gases such as hydrogen and helium do not absorb electromagnetic radiation in the visible or infrared region of the spectrum. However, at sufficiently high gas densities, *collisionally interacting pairs* of nonpolar molecules, such as $H_2$-$H_2$ or $H_2$-He, absorb noticeably in these spectral regions as Welsh and his associates have shown.[1] The absorption is caused by a dipole moment induced by intermolecular interactions.[2,3] Three mechanisms contribute to the induced dipole: the polarization of the collisional partner $X$ (which, for example, may be a He atom or a $H_2$ molecule) in the quadrupole field of another molecule ($H_2$); electron exchange in the supermolecule $H_2$-$X$ at near range; and dispersion interaction. The induction processes are well understood[4,5] and have been studied theoretically and by *ab initio* calculations of supermolecules such as $H_2$-$X$.[6–13]

Once the induced dipole moment $\boldsymbol{\mu}=\boldsymbol{\mu}(\mathbf{R};\ r_{H_2}, r_X, \Omega_{H_2}, \Omega_X)$ is known as a function of the $H_2$-$X$ separation $R$, the vibrational coordinates $r_{H_2}$ of $H_2$ and $r_X$ of $X$ (if $X$ is a molecule), the collision-induced-absorption (CIA) spectra can be computed quite rigorously.[14,15] If state-of-the-art induced dipole moments are input that are obtained from highly correlated wave functions, a very close agreement of measured CIA spectra with *ab initio* computations is observed.[12,13,16,17] Not only do the shapes of the calculated and measured spectral profiles agree. All recent measurements of CIA spectra of $H_2$-$H_2$ and $H_2$-He have been calibrated in units of absolute intensities and measured and computed spectra have been shown to agree on an absolute intensity scale with root-mean-square deviations of just a few percent.

We note that various kinds of CIA spectra are known.[1] Besides the translational spectra of the supermolecule $H_2$-$X$ which leave the rotovibrational states of the participating collisional partners unchanged, purely rotational CIA spectra have been observed which leave the vibrational states of $H_2$ and $X$ unchanged. Vibrational transitions in either $H_2$ or $X$ (if $X$ is a molecule) may occur which lead to rotovibrational (RV) CIA spectra. These may be in the fundamental band ($v=0$, $v'=1$), or in overtone or "hot" bands ($v'>1$, $v>0$). Simultaneous transitions in both partners may also occur at sums and differences of the RV frequencies of the molecules involved. Several of these CIA spectra of $H_2$-$X$ pairs are of considerable significance in astrophysics, especially in more or less neutral and dense environments, such as the atmospheres of the outer planets,[1,18–21] late stars,[22–24] certain white dwarfs,[25,26] and the hypothetical "population III" stars.[27,28] The computation of such spectra from first principles can be done with precision and is therefore a valuable, indeed a necessary supplement to the data required for the study of such atmospheres, because laboratory data are usually subject to some technical limitation of temperature or absorption path length.

The rototranslational (RT) CIA spectra in the far infrared of $H_2$-$H_2$ and $H_2$-He pairs have been accurately obtained from first principles.[12,13,29] Since such computa-

 

tions are involved and cannot readily be repeated elsewhere, the results of the exact quantum calculations have been approximated by simple analytical functions that can be computed in seconds on small computers. These represent the spectra over a wide range of temperatures and frequencies closely.[30,31] However, in our attempts to extend such work to the RVCIA spectra in the near infrared, somewhat unexpectedly we encountered serious problems to be described next.

The CIA spectra arise from dipole transitions between accessible states of the supermolecule $H_2$-$X$. The computation of the translational wave function requires the knowledge of the $H_2$-$X$ interaction potential. It is well known that the interaction potential depends not only on the separation $\mathbf{R}$ of the pair (and the orientations $\Omega_{H_2}$ and $\Omega_X$ of the partners), but also on the vibrational coordinates $r_{H_2}$ and $r_X$ (if $X$ is a molecule). In other words, the translational wave function of the final state must be computed from an interaction potential that differs from that of the initial state of the complex, especially if RV transitions are considered. While the vibrational averages of the interaction potential $V(\mathbf{R},\Omega_{H_2},\Omega_X,r_{H_2},r_X)$ for various vibrational states may not seem to differ drastically, they differ enough at near range, $R\sim\sigma$ where $\sigma$ is the collision diameter, to render the first spectral moment of the fundamental hydrogen band about 20% greater at temperatures from 200 to 300 K, and even more at higher temperatures, relative to the values obtained if the same potential is assumed for the initial and final states of the pair.[32(a)] For the the overtone bands much greater corrections are observed[32(b)] and the line shapes computed with and without accounting for the variation of the interaction potential with the vibrational states differ strikingly, especially at high temperatures. We mention, though, that the zeroth moments remain unaffected.[32(a)]

Perhaps more surprising, we found the existing modeling functions commonly employed in such work[15,33–35] to be not accurate, indeed in several instances quite inaccurate for the modeling of the RVCIA spectra. We shall show that this problem is also related to the fact that interaction potentials depend on the vibrational states of the molecules involved. This $v$ dependence (as we will call it for brevity) renders the individual line profiles [for example, those of the usually prominent, "forbidden" $S_{\Delta v}(J)$ lines of $H_2$] inconsistent with a profile satisfying a form of the detailed balance condition widely employed. The symmetry of the line profiles of RVCIA spectra is the subject of this paper, which may be considered an extension and refinement of previous work[14] concerning the theory of CIA spectra.

## II. THEORY

In the low-density limit, for example, when intercollisional interference and other many-body effects are neglected, the spectral distribution is determined solely by the dynamics of a pair of molecules. In this first and widely used approximation,[1,34,35] the intermolecular potential has been assumed to be independent of the internal motion of the molecules: the potential depends only on the intermolecular separation, so that the translational motion is fully decoupled from the internal motion of the molecules. In this case, the collision-induced spectral density may be described as a convolution of a translational spectrum with a "stick spectrum" whose lines are placed in correspondence with the RV transitions. The translational spectrum is computed by solving numerically the radial Schrödinger equation with the isotropic intermolecular potential that is a function of the intermolecular separation only[34,36,37] and satisfies a detailed balance condition [Eq. (19) below].

To a better approximation, the intermolecular potential can be considered to be dependent on the vibrational and translational variables (but not on the rotational ones). Moreover, in systems involving $H_2$, the vibrational variables may be considered as changing with time much faster than the translational ones, so that the motion of the latter can be determined by an isotropic potential that is the vibrational average of the potential associated with the appropriate vibrational state. The resulting translational spectrum does not possess, however, the same properties as the one in which the coupling between translations and vibrations is neglected. In fact, as we shall show, this new line shape cannot be expected to satisfy the "detailed balance condition," Eq. (19), below.

Under the circumstances, the symmetry of RV line profiles and the model line shapes representing them is reconsidered. In this paper we suggest a method to construct analytical profiles of the proper symmetry to represent RV spectra of systems such as $H_2$-$H_2$ and $H_2$-He. It will be seen that the modifications we suggest with respect to previously proposed models are particularly important at high temperatures and for overtone and hot bands ($v'>1$, $v=0$, and $v'>v>0$, respectively) in general.

We define the spectral density $g(\bar{\omega})$ as[14]

$$g(\bar{\omega})=\sum_{s,s'}P_s\,|\langle s\,|\,\boldsymbol{\mu}\,|\,s'\rangle|^2\delta(\bar{\omega}-\omega_{ss'})\ . \tag{1}$$

In this expression, $s$ and $s'$ indicate the initial and final states of the supermolecule, $P_s$ is the probability of occupation of the state $s$, $\boldsymbol{\mu}$ is the dipole moment induced by intermolecular interactions, $\bar{\omega}$ is the angular frequency, $\omega_{ss'}=(E_{s'}-E_s)/\hbar$, and $E_s$ is the energy of state $|s\rangle$. The absorption coefficient $\alpha(\bar{\omega})$ of a collisional pair is expressed in terms of the spectral density, according to

$$\alpha(\bar{\omega})=\rho_{H_2}\rho_X\frac{4\pi^2n_L^2}{3\hbar c}\bar{\omega}(1-e^{-\hbar\bar{\omega}/kT})Vg(\bar{\omega})\ . \tag{2}$$

Equation (2) describes the enhancement spectra of the mixture of hydrogen and rare-gas pairs. The $\rho_{H_2}$ and $\rho_X$ designate the density, in amagats, of hydrogen and the rare gas, respectively. We note that the factor $\rho_{H_2}\rho_X$ must be replaced by $\frac{1}{2}\rho_{H_2}^2$ if absorption in pure hydrogen is considered. $V$ designates the volume and $n_L$ is Loschmidt's number.

Since we will regard the molecules as rotating freely, it is convenient to expand the spherical components of the induced dipole moment $\boldsymbol{\mu}$ in terms of angular functions,

$$\Psi_{1v}^{(c)}=\frac{4\pi}{\sqrt{3}}\sum_{\mu,M}C(\lambda L1;\mu M v)Y_{\lambda\mu}(\Omega_{H_2})Y_{LM}(\Omega)\ , \tag{3}$$

$$\Psi_{1\nu}^{(c)}=\left[\frac{(4\pi)^3}{3}\right]^{1/2}\sum_{\mu,M}C(\Lambda L1;\mu M\nu)\times\sum_{\mu_1,\mu_2}C(\lambda_1\lambda_2\Lambda;\mu_1\mu_2\mu)\times Y_{\lambda_1\mu_1}(\Omega_{H_2})\times Y_{\lambda_2\mu_2}(\Omega_X)Y_{LM}(\Omega)\ , \quad (4)$$

depending on whether $X$ is an atom or diatomic molecule. The superscript $(c)$ designates the set of expansion parameters $\{\lambda,L\}$ if $X$ is an atom [Eq. (3)] and $\{\lambda_1,\lambda_2,L,\Lambda\}$ if $X$ is a diatomic molecule [Eq. (4)]. The $C$ ( ; ) are Clebsch-Gordan coefficients and the $Y_{\lambda\mu}$ are spherical harmonics. The direction of the intermolecular axis in a laboratory fixed frame is called $\Omega$. In terms of Eqs. (3) and (4), the spherical components (with $\nu=0,\pm1$) of the induced dipole component $\mu$ can be written as[38,39]

$$\mu_{1\nu}=\sum_{(c)}A^{(c)}(R,r_{H_2},r_X)\Psi_{1\nu}^{(c)}\ , \quad (5)$$

with coefficients $A^{(c)}$ that have been defined previously in a slightly different notation, according to

$$A^{(c)}(R,r_{H_2})=A_{\lambda L}(R,r_{H_2})\ , \quad (6)$$

$$A^{(c)}(R,r_{H_2}r_X)=A_\Lambda(\lambda_1\lambda_2L;R,r_{H_2}r_X)\ , \quad (7)$$

depending on whether Eq. (3) or (4) is considered.

As a consequence of the assumed independence of the intermolecular potential on the rotational variables, any state $|s\rangle$ of the supermolecule can be written as the product of a state representing the free rotation of the molecules, $|r,m_r\rangle$, and one describing both vibrational and translational variables, $|\Phi\rangle$, according to

$$|s\rangle=|r,m_r\rangle\,|\phi\rangle\ . \quad (8)$$

That is, we disregard any coupling between rotational states on the one hand and vibrational and translational on the other. In Eq. (8), $m_r$ designates a set of quantum numbers which distinguishes among all states with the same rotational energy $E_r$. Upon making use of Eq. (8) in Eq. (1), the sum over $r,m_r,r',m_r'$ can be computed and we get

$$Vg(\bar\omega)=\sum_{(c),r,r'}a_{r,r'}^{(c)}F^{(c)}(\bar\omega-\omega_{r,r'})\ . \quad (9)$$

In other words, the spectral function is written as a sum over various line profiles centered at the rotational transition frequencies $\omega_{r,r'}$. For each set of expansion parameters $(c)$, the quantities $a_{r,r'}^{(c)}$ satisfy the selection rules appropriate for the $(c)$ component, and are chosen such that

$$\sum_{r'}a_{r,r'}^{(c)}=P_r,\quad \sum_{r,r'}a_{r,r'}^{(c)}=1\ , \quad (10)$$

where $P_r$ is the population probability of the rotational state $|r\rangle$. We thus get

$$V\int_{-\infty}^{\infty}g(\bar\omega)d\bar\omega=\sum_{(c)}\int_{-\infty}^{\infty}F^{(c)}(\bar\omega)d\bar\omega\ . \quad (11)$$

The line-profile functions $F^{(c)}(\bar\omega)$ may be written as

$$F^{(c)}(\bar\omega)=\sum_{\phi,\phi'}VP_\phi\frac{4\pi}{2L+1}\sum_M|\langle\phi|A^{(c)}(R,r_{H_2}r_X)Y_{LM}(\Omega)|\phi'\rangle|^2\delta(\bar\omega-\omega_{\phi\phi'})\ . \quad (12)$$

Next, we assume that the states $|\phi\rangle$ and $|\phi'\rangle$ are of the form

$$|\phi\rangle=|v\rangle\,|\tau\rangle_v\ , \quad (13)$$

$$|\phi'\rangle=|v'\rangle\,|\tau'\rangle_{v'}\ , \quad (14)$$

with $|v\rangle$ and $|v'\rangle$ designating the initial and final vibrational states of the pair, $|\tau\rangle_v$ and $|\tau'\rangle_{v'}$ the translational eigenstates of the Hamiltonians $\langle v|H|v\rangle$ and $\langle v'|H|v'\rangle$ whose eigenvalues are the energies $E_\tau$ and $E_{\tau'}$, respectively. The Hamiltonian $H$ is the total Hamiltonian of the pair *minus* the rotational and vibrational kinetic energies of the molecules.

If a transition from the initial state $v$ to the final state $v'$ takes place, we get, from Eq. (12),

$$F_{vv'}^{(c)}(\omega)=P_v\sum_{\tau,\tau'}V\frac{4\pi}{2L+1}P_\tau\times\sum_M|{}_v\langle\tau|B_{vv'}^{(c)}(R)Y_{LM}(\Omega)|\tau'\rangle_{v'}|^2\times\delta(\omega-\omega_{\tau\tau'})\ , \quad (15)$$

where $\omega=\bar\omega-\omega_{vv'}$ is the frequency shift relative to the line center $\omega_{vv'}$, and

$$B_{vv'}^{(c)}=\langle v|A^{(c)}(R,r_{H_2}r_X)|v'\rangle \quad (16)$$

is the vibrational transition matrix element of the induced dipole. $P_v$ and $P_\tau$ designate the population probabilities of the initial vibrational and translational states, $|v\rangle$ and $|\tau\rangle$, respectively. Equation (15) is formally the same as one derived previously,[14] but the radial part of the translational wave function of initial and final states is now computed with the vibrational average of the interaction potential,

$$V_v(R)=\langle v|V_0(R,r_{H_2}r_X)|v\rangle\ , \quad (17)$$

and similarly for $v'$. The interaction potentials for initial and final states thus differ if $v\neq v'$. Using numerical methods, the spectral line profiles, Eq. (15), of the fundamental band have previously been computed for $H_2$-He pairs[17] with the use of the *ab initio* potential of Meyer *et al.*[40] The spectra calculated with and without accounting for the dependence on the vibrational coordinates $r_{H_2}$ were found to differ significantly. The measurements at temperatures from 18 to $\sim$300 K could be shown to be modeled much more closely by the profile obtained with accounting for the $v$ dependence.

Since the computations of quantum profiles according to Eq. (15) are somewhat complex, it is common practice to substitute for an exact quantum profile $F(\omega)$ a simple, analytical profile, $\Gamma(\omega;\tau_1\tau_2\cdots)$ with adjustable parameters $\tau_i$, which may approximate exact profiles closely, provided the $N$ parameters are chosen so that $N$ spectral moments of $F$ and $\Gamma$ are matched,

$$\frac{1}{P_v}\int_{-\infty}^{\infty} F(\omega)\omega^n d\omega = \int_{-\infty}^{\infty} \Gamma(\omega)\omega^n d\omega \tag{18}$$

for $0\le n\le N-1$. The resulting representation was shown to be surprisingly accurate for a wide selection of RTCIA spectra,[31,41] but an extension to RVCIA spectra was *unworkable* after the momentum expressions input were chosen to account for the $v$ dependence.[32(a)] Only with the assumption $V_v(R)\equiv V_{v'}(R)$ could a spectrum thus be modeled which, however, was a poor approximation of measurements and of exact computations if $v\neq v'$. The reason for this somewhat unexpected observation is related to the *significantly different symmetry* of the profiles $F(\omega)$ and $\Gamma(\omega)$ observed in the vibrational bands which we will discuss next.

As far as we know, functions $\Gamma(\omega)$ that have been considered in the past as a model line shape[33,15] have all been chosen to satisfy a detailed balance condition,

$$\Gamma(-\omega)=e^{-\hbar\omega/kT}\Gamma(\omega)\ , \tag{19}$$

where $\omega$ designates the frequency shift relative to the transition frequency. (We ignore here the classical profiles which are symmetric and thus not suitable to model hydrogen systems at low temperatures.) It is noteworthy that the exact line profiles $F_{vv'}(\omega)$ do *not* satisfy such a symmetry relation, Eq. (19), unless $v=v'$ (as is the case in the RT band). In fact, because $\delta(-\omega-\omega_{\tau\tau'})=\delta(\omega-\omega_{\tau'\tau})$, replacing $\omega$ by $-\omega$ is equivalent to exchanging $\tau$ and $\tau'$ in Eq. (15), except in the $\delta$ function. $P_{\tau'}$ equals $\exp(-\hbar\omega/kT)P_\tau$, but the square modulus of the matrix elements remains the same only if the initial and final vibrational states are the same (or if the translational motion does not depend on the vibrational state). The fact is that $F(\bar\omega)$ satisfies the detailed balance condition for inversion of the *absolute* frequency $\bar\omega$, not of the frequency shift $\omega$. The inversion of the frequency shift $\omega$ in Eq. (15) by contrast, simply means that we are going from $\bar\omega=\omega_{vv'}+\omega$ to $\bar\omega=\omega_{vv'}-\omega$. The inversion of the frequency $\bar\omega$, on the contrary, is actually equivalent to inverting both $\omega$ and $\omega_{vv'}$: $-\bar\omega=\omega_{v'v}-\omega$. In fact, starting from Eq. (15), it can readily be shown that

$$\frac{F_{v'v}(-\omega)}{P_{v'}}=e^{-\hbar\omega/kT}\frac{F_{vv'}(\omega)}{P_v}\ , \tag{20}$$

which differs substantially from Eq. (19) if $v\neq v'$. The profile $F_{vv'}$ on the right-hand side of Eq. (20) is associated with the vibrational transition $v\to v'$, while the $F_{v'v}$ to the left designates the profile associated with the inverse transition, $v'\to v$. The RVCIA spectra should be modeled with the help of profiles which satisfy Eq. (20), not Eq. (19). These can be constructed from the familiar models $\Gamma$ as we will show next.

## III. RV MODEL PROFILES

Spectral profiles $K^{(c)}_{vv'}(\omega)=F^{(c)}_{vv'}(\omega)/P_v$ suitable for modeling RVCIA spectra should be consistent with Eq. (20). The present known, successful model profiles[34,15] $\Gamma$ satisfy Eq. (19) but not Eq. (20). In order to benefit from the wealth of information obtained for the existing successful models and, at the same time, satisfy Eq. (20), we shall briefly consider how suitable model functions $K$ can be constructed from the familiar $\Gamma$ so that Eq. (20) is satisfied.

We define the functions $X(\omega)$ and $Y(\omega)$ such that

$$X^{(c)}(-\omega)=e^{-\hbar\omega/kT}X^{(c)}(\omega)\ , \tag{21}$$

$$Y^{(c)}(-\omega)=-e^{-\hbar\omega/kT}Y^{(c)}(\omega)\ , \tag{22}$$

and construct an RV model profile from these, according to

$$K^{(c)}_{vv'}(\omega)=X^{(c)}(\omega)+Y^{(c)}(\omega)\ . \tag{23}$$

This is always possible. It is sufficient to choose

$$X^{(c)}(\omega)=\tfrac{1}{2}[K^{(c)}_{vv'}(\omega)+e^{\hbar\omega/kT}K^{(c)}_{vv'}(-\omega)]\ , \tag{24}$$

$$Y^{(c)}(\omega)=\tfrac{1}{2}[K^{(c)}_{vv'}(\omega)-e^{\hbar\omega/kT}K^{(c)}_{vv'}(-\omega)]\ . \tag{25}$$

With the help of Eq. (20), we write these as

$$X^{(c)}(\omega)=\tfrac{1}{2}[K^{(c)}_{vv'}(\omega)+K^{(c)}_{v'v}(\omega)]\ , \tag{26}$$

$$Y^{(c)}(\omega)=\tfrac{1}{2}[K^{(c)}_{vv'}(\omega)-K^{(c)}_{v'v}(\omega)]\ . \tag{27}$$

The $X$ and $Y$ can thus be expressed in terms of the profiles of the up and the associated down ($v'\leftrightarrow v$) transitions. The spectral moments of $X$ and $Y$ can thus be written as a simple combination of the moments of the up and down transitions. These can be computed from induction operator and interaction potential.[32(a)] Furthermore, the function $X$, Eq. (21), satisfies the condition, Eq. (19), and is conveniently represented by one of the familiar models, $\Gamma$. A simple choice for $Y^{(c)}(\omega)$ could be $(\omega/\Delta)\Gamma'(\omega)$ where $\Delta$ is a constant to be specified below, and $\Gamma'$ is another model function which satisfies Eq. (19). In other words, according to Eq. (23), the RV profiles $K$ can be represented by two familiar model functions, $\Gamma$ and $\Gamma'$, whose parameters may be defined from the computable spectral moments of $K_{vv'}$ and $K_{v'v}$.[32]

The parameters $\tau_1\cdots\tau_N$ of the function $\Gamma$, and $\tau'_1\cdots\tau'_N$ of $\Gamma'$, can be determined by matching the spectral moments of the model functions and those of the $X^{(c)}, Y^{(c)}$ given by Eqs. (26) and (27); the moments of $X$ and $Y$ are called $M^{(c)}_{Xn}$ and $M^{(c)}_{Yn}$, respectively. We give here the first three moments of $X$ which are readily obtained from Eq. (26) and Refs. 42 and 32(a),

$$M^{(c)}_{X0}=\int |B|^2\frac{g_v+g_{v'}}{2}d^3\mathbf{R}\ , \tag{28}$$

$$M^{(c)}_{X1}=\frac{\hbar}{2\mu}\int\left[(B^{\mathrm{I}})^2+L(L+1)\frac{|B|^2}{R^2}\right]\frac{g_v+g_{v'}}{2}d^3\mathbf{R}+\frac{1}{\hbar}\int |B|^2(V_{v'}-V_v)\frac{g_v-g_{v'}}{2}d^3\mathbf{R}\ , \tag{29}$$

$$M_{X2}^{(c)}=\frac{\hbar^2}{\mu^2}\int\left[-\tfrac{1}{4}BB^{\mathrm{IV}}-\tfrac{1}{2}B^{\mathrm{I}}B^{\mathrm{III}}+\frac{L(L+1)}{2R^2}(B^{\mathrm{I}})^2-\frac{L(L+1)}{R^3}BB^{\mathrm{I}}+\frac{L^2(L+1)^2}{4R^4}B^2\right]\frac{g_v+g_{v'}}{2}d^3\mathbf{R}$$
$$+\frac{1}{\mu}\int\left[BB^{\mathrm{I}}\frac{g_vV_v^{\mathrm{I}}+g_{v'}V_{v'}^{\mathrm{I}}}{2}+2BB^{\mathrm{II}}\frac{g_vV_v+g_{v'}V_{v'}}{2}\right]d^3\mathbf{R}-\frac{2}{\mu}\int BB^{\mathrm{II}}\frac{g_v^{(E)}+g_{v'}^{(E)}}{2}d^3\mathbf{R}$$
$$+\frac{1}{\mu^2}\int\left[\frac{BB^{\mathrm{II}}}{R^2}-\frac{BB^{\mathrm{I}}}{R^3}+\frac{L(L+1)}{2R^4}B^2\right]\frac{g_v^{(M)}+g_{v'}^{(M)}}{2}d^3\mathbf{R}+\frac{1}{\hbar^2}\int B^2(V_{v'}-V_v)^2\frac{g_v+g_{v'}}{2}d^3\mathbf{R}$$
$$+\frac{1}{\mu}\int\left[(B^{\mathrm{I}})^2+\frac{L(L+1)}{R^2}B^2\right](V_{v'}-V_v)\frac{g_v-g_{v'}}{2}d^3\mathbf{R}+\frac{1}{\mu}\int BB^{\mathrm{I}}(V_{v'}^{\mathrm{I}}-V_v^{\mathrm{I}})\frac{g_v-g_{v'}}{2}d^3\mathbf{R}\ . \tag{30}$$

The moments $M_{Yn}^{(c)}$ of $Y$ are obtained from similar expressions simply by changing the signs of all $g_{v'}$, $g_{v'}^{(E)}$, and $g_{v'}^{(M)}$ that appear in Eqs. (28)–(30), so that we need not repeat the expressions here. We note that the reduced mass was designated $\mu$, $B$ is short for $B_{vv'}^{(c)}(R)$, and $V_v$ and $V_{v'}$ are the vibrational averages, Eq. (17), of the isotropic interaction potential of initial and final states, respectively. Superscripted Roman numericals I, II, etc. mean first, second, etc. derivatives with respect to $R$. The radial distribution function $g=g(R)$ depends on the interaction potentials $V_v, V_{v'}$ and is thus subscripted like the potentials; the low-density limit of the distribution function will be sufficient for our purposes. The functions $g^{(E)}$ and $g^{(M)}$ are the same as $G_E$ and $G_M$ of Ref. 42. The notation $\int f(R)d^3\mathbf{R}$ means $4\pi\int_0^\infty f(R)R^2dR$ as usual.

For each profile $K_{vv'}^{(c)}(\omega)$, the spectral moments $M_{vv';n}^{(c)}$, with $n=0,1,2$, can be calculated from a quantum or semiclassical formalism as described elsewhere;[32(a)] see also Refs. 42 and 43. From Eqs. (26) and (27) it is obvious that these are related to the $M_{Xn}$ according to

$$M_{Xn}^{(c)}=\tfrac{1}{2}(M_{vv';n}^{(c)}+M_{v'v;n}^{(c)})\ , \tag{31}$$

and similarly, with the plus sign replaced by a *minus*, for $M_{Yn}^{(c)}$. Once the $M_{Xn}^{(c)}$ and $M_{Yn}^{(c)}$ are obtained, the functions $X^{(c)}(\omega)$, $Y^{(c)}(\omega)$ and thus $K_{vv'}^{(c)}(\omega)$ and $F_{vv'}^{(c)}(\omega)$ can be modeled with the help of familiar profiles $\Gamma$, $\Gamma'$ that depend on three parameters. Existing model profiles are usually normalized so that their zeroth moment equals unity. In this case,

$$X(\omega)=\Gamma(\omega)M_{X0}\ . \tag{32}$$

The remaining two parameters of $\Gamma$, $\tau_1$ and $\tau_2$, are determined by solving the equations

$$\int_{-\infty}^{\infty}\Gamma(\omega;\tau_1\tau_2)\omega\,d\omega=\frac{M_{X1}}{M_{X0}}\ , \tag{33}$$

$$\int_{-\infty}^{\infty}\Gamma(\omega;\tau_1\tau_2)\omega^2d\omega=\frac{M_{X2}}{M_{X0}}\ . \tag{34}$$

As mentioned above, $Y(\omega)$ may be modeled with the help of a function

$$Y(\omega)=\frac{\omega}{\Delta}\Gamma'(\omega;\tau_1'\tau_2')M_{Y0}\ . \tag{35}$$

In this case, we get

$$\int_{-\infty}^{\infty}\Gamma'(\omega;\tau_1'\tau_2')\omega\,d\omega=\Delta\ , \tag{36}$$

$$\frac{1}{\Delta}\int_{-\infty}^{\infty}\Gamma'(\omega;\tau_1'\tau_2')\omega^2d\omega=\frac{M_{Y1}}{M_{Y0}}\ , \tag{37}$$

$$\frac{1}{\Delta}\int_{-\infty}^{\infty}\Gamma'(\omega;\tau_1'\tau_2')\omega^3d\omega=\frac{M_{Y2}}{M_{Y0}}\ , \tag{38}$$

which determine $\tau_1'$, $\tau_2'$, and $\Delta$. The functions $X$ and $Y$, and thus $K$, Eq. (23), are fixed in this way from the generalized moment relations, Eqs. (28)–(30), once the models $\Gamma$ and $\Gamma'$ are chosen. $K$ satisfies Eq. (20) as RV profiles should. The only question remaining at this point is which of the known functions $\Gamma$ and $\Gamma'$ to select for an optimal representation of the exact profile, Eq. (15). Such studies are under way and may currently be summarized by stating that for the RVCIA profiles, the Birnbaum-Cohen (BC) and $K_0$ models[33,31] seem to work quite well for multipolar induction and overlap induction, respectively. We note that the left-hand sides of Eqs. (33)–(38) are simple algebraic functions of the parameters $\tau_i$ and $\tau_i'$ if BC or $K_0$ models are chosen for the $\Gamma$ and $\Gamma'$; see Refs. 30 and 31 for the details.

## IV. NUMERICAL COMPUTATIONS

For the $H_2$-He systems, an accurate *ab initio* interaction potential[40] exists that specifies the variation with the vibrational coordinate $r_{H_2}$. That potential has been used to compute exact quantum profiles in close agreement with existing measurements of the RVCIA spectra of the fundamental band ($v=0$, $v'=1$).[17] Such spectra can be computed from theory if each line profile is calculated directly from the quantum formalism at both positive and negative frequency shifts [i.e., without computing the profile at negative shifts from Eq. (19) as was done for the RTCIA spectra in order to save computer time]. Alternatively, the "red" wings of the profiles can be obtained from the "blue" wings with the help of Eq. (20). Such computational results will be briefly called "exact" profiles.

For the fundamental band ($v=0\rightarrow v'=1$), we have computed over a range of temperatures from 18 to 7000 K the lowest three spectral moments $M_{vv';n}^{(c)}$ and $M_{v'v;n}^{(c)}$ of the exact profiles $K_{vv'}^{(c)}(\omega)$. For this purpose, we used the sum formulas given elsewhere[32] that account for the $v$ dependence of the interaction potential. The lowest three

moments are shown in Figs. 1–4 for two representative induction components: $\lambda L = 01$ (isotropic overlap induction term) and 23 (quadrupolar induction term); the anisotropic overlap term (21) and the hexadecapolar induction term (45) are very similar to the 01 and 23 components, respectively, and are not shown. The solid line represents the exact quantum calculations as described in Ref. 43 but modified to account for the $v$ dependence of the potential.[32(a)] The dash-dot line shows the results obtained with the assumption $V_v \equiv V_{v'}$ (with $v=0$), which neglects the $v$ dependence. Figures 1 and 2 show the moments for the "up" transitions, $v=0 \rightarrow v'=1$, while Figs. 3 and 4 give the moments associated with the inverse transitions, $v' \rightarrow v$, as needed for this purpose; see Eq. (31).

The zeroth moments are not affected by the $v$ dependence, but the others, especially the first moments, differ substantially, the more so the higher the temperature. As might be expected, the overlap components are more strongly affected than the multipolar induction terms which are more long range than the former. We note that these moments $M^{(c)}_{01;n}$, obtained directly from induction operators and potential, agree to within 1% with the moments obtained by integrating the exact lines shapes, multiplied by $\omega^n$, over frequency.

Since classical line shapes have vanishing odd moments, and since the $v$ dependence is significant mainly for the first moments but leaves the second moments nearly unaffected, this $v$ dependence apparently is of quantum nature. However, contrary to the more familiar quantum corrections,[43–45] this one is *increasing* with temperature.

The first moments of the inverse transition, Figs. 3 and 4, show a steep falloff and even a change of sign (not shown) at high temperature. That fact is related to factors such as $(V_v - V_{v'})$ that occur in certain terms of the sum formulas,[32] and poses no problems for the purpose at hand.

We have also modeled the $\lambda L = 01$ and 23 line profiles using the formalism suggested above. For this example, we represent the function $X$ by the $K_0$ shape[46] for $\lambda L = 01$ in Fig. 5 and the BC shape[33] for $\lambda L = 23$ in Fig. 6. We take function $Y$ in the form of Eq. (35), with $\Gamma'$ given by a BC function,[33]

$$Y(\omega) = \exp\left[-\frac{\tau_1' - |\tau_2'|}{\tau_1'}\right]\frac{\tau_1'|\tau_2'|}{\tau_0}\omega\Gamma_{\mathrm{BC}}(\omega)M_{Y0}\ , \quad (39)$$

where $\tau_0 = \hbar/(2kT)$, $k$ is the Boltzman factor, and $T$ is the temperature. The parameters $\tau_1'$ and $\tau_2'$ are obtained by solving Eqs. (37) and (38), which in the case of a BC shape reduce to

$$\frac{M_{Y1}}{M_{Y0}} = \frac{\tau_0}{\tau_1'|\tau_2'|} + \frac{\tau_0}{(\tau_2')^2} + \frac{1}{\tau_0}\ , \quad (40)$$

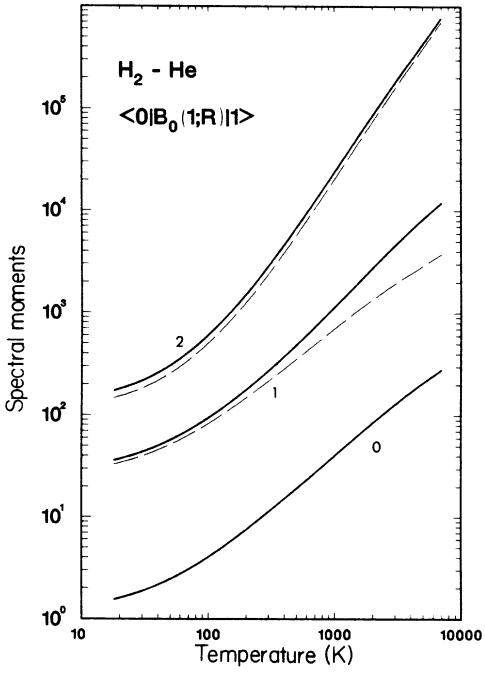


FIG. 1. Spectral moments $M^{01}_{vv';n}$ of the isotropic component ($\lambda L = 01$) are shown as a function of temperature for the fundamental band ($v=0 \rightarrow v'=1$) (solid line). The zeroth moment ($n=0$, at the bottom) is given in units of $10^{-64}$ ergs, the first moment ($n=1$, center) in units of $10^{-52}$ ergs s$^{-1}$, and the second moment ($n=2$, at the top) in units of $10^{-39}$ ergs s$^{-2}$. Also shown are the values of the moments computed neglecting the $v$ dependence (dash-dot line).

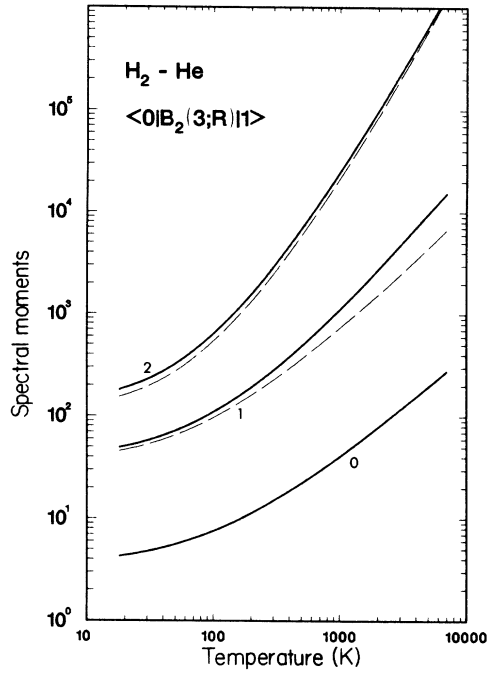


FIG. 2. Spectral moments $M^{23}_{vv';n}$ of the quadrupole-induced component ($\lambda L = 23$) are shown as a function of temperature for the fundamental band ($v=0 \rightarrow v'=1$) (solid line). The zeroth moment ($n=0$, at the bottom) is given in units of $10^{-65}$ ergs, the first moment ($n=1$, center) in units of $10^{-53}$ ergs s$^{-1}$, and the second moment ($n=2$, at the top) in units of $10^{-40}$ ergs s$^{-2}$. Also shown are the values of the moments computed neglecting the $v$ dependence (dash-dot line).

$$\frac{M_{Y2}}{M_{Y0}}=\frac{3}{\tau_1'|\tau_2'|}+\frac{3\tau_0^2}{\tau_1'|\tau_2'|^3}+\frac{\tau_0^2}{(\tau_1')^2(\tau_2')^2}+\frac{3}{(\tau_2')^2}+\frac{3\tau_0^2}{(\tau_2')^4}\ . \tag{41}$$

It is useful to introduce

$$x=\frac{M_{Y1}}{M_{Y0}}-\frac{1}{\tau_0}\ ,$$

$$y=\left[\frac{4M_{Y2}}{M_{Y0}}-\frac{3M_{Y1}^2}{M_{Y0}^2}-\frac{6M_{Y1}}{\tau_0 M_{Y0}}+\frac{9}{\tau_0^2}\right]^{1/2}\ .$$

With these, for $-x-y>0$, we have

$$\frac{1}{(\tau_2')^2}=\frac{-x-y}{2\tau_0}\ , \tag{42}$$

$$\frac{1}{\tau_1'|\tau_2'|}=\frac{3x+y}{2\tau_0}\ , \tag{43}$$

while for $-x+y>0$, we get

$$\frac{1}{(\tau_2')^2}=\frac{-x+y}{2\tau_0}\ , \tag{44}$$

$$\frac{1}{\tau_1'|\tau_2'|}=\frac{3x-y}{2\tau_0}\ . \tag{45}$$

Relationships for the computation of the parameters $\tau_1,\tau_2$ to model the functions $\Gamma$ and $X$ have been communicated previously.[31] The models thus obtained are referred to as the "$v$-dependent models." These are plotted in Figs. 5 and 6 using the dotted line. For the $\lambda L=01$ component, this $v$-dependent model is nearly indistinguishable from the exact profile (solid line), and for the $\lambda L=23$ component a close approximation, especially near the line center, is observed.

Figures 5 and 6 also compare the $v$-dependent models with the previously used "$v$-independent" BC or $K_0$ shapes that satisfy Eq. (19). While the former are in agreement with the exact profiles at all frequencies, the latter differ strikingly for both the isotropic overlap component [which is the main contribution to the $Q_1(J)$ branch] and the quadrupole-induced component [which generate much of the $S_1(J)$ line intensities]. Similar plots at much lower temperature ($T<100$ K) reveal lesser differences (not shown). At higher temperature ($T>600$ K) the equations which determine the parameters for a $v$-independent modeling have no solutions if the $v$-dependent spectral moments are input.[32(a)] If, on the other hand, model profiles are chosen which satisfy Eq. (19), or if classical modeling is attempted neglecting all $v$-dependences, the results do not approximate very well the exact profiles of RVCIA spectra at high temperatures

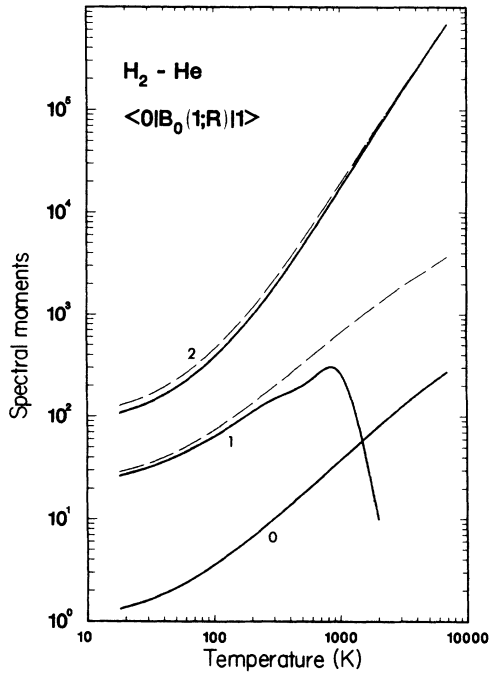


FIG. 3. Spectral moments $M_{vv';n}^{01}$ of the isotropic component ($\lambda L=01$) are shown as a function of temperature for the inverse transitions ($v=1\rightarrow v'=0$) (solid line). The zeroth moment ($n=0$, at the bottom) is given in units of $10^{-64}$ ergs, the first moment ($n=1$, center) in units of $10^{-52}$ ergs s$^{-1}$, and the second moment ($n=2$, at the top) in units of $10^{-39}$ ergs s$^{-2}$. At the higher temperatures, the first moment falls off steeply and changes sign (truncated in the figure). Also shown are the values of the moments computed neglecting the $v$ dependence (dash-dot line).

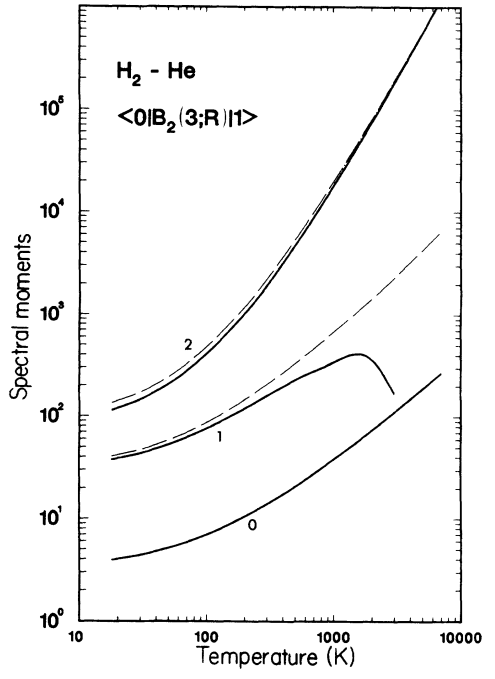


FIG. 4. Spectral moments $M_{vv';n}^{23}$ of the quadrupole-induced component ($\lambda L=23$) are shown as a function of temperature for the inverse transition ($v=1\rightarrow v'=0$) (solid line). The zeroth moment ($n=0$, at the bottom) is given in units of $10^{-65}$ ergs, the first moment ($n=1$, center) in units of $10^{-53}$ ergs s$^{-1}$, and the second moment ($n=2$, at the top) in units of $10^{-40}$ ergs s$^{-2}$. At the higher temperatures, the first moment falls off steeply and changes sign (truncated in the figure). Also shown are the values of the moments computed neglecting the $v$ dependence (dash-dot line).

(not shown). Spectra at the higher temperatures are of interest for the atmospheres of cool stars and analytical profiles employed for studies related to stellar atmospheres should satisfy Eq. (20).

In conclusion, we raise the question: how badly is the detailed balance condition, Eq. (19), violated in the fundamental band of $H_2$-He pairs? Figure 7 provides an answer. For the $\lambda L = 01$ (overlap) and 23 (quadrupolar) components, from exact-line-shape computations we determine the quantity

$$Q = \frac{F_{01}^{(\lambda L)}(\omega_0)}{F_{01}^{(\lambda L)}(-\omega_0)} e^{-\hbar\omega_0/kT} \tag{46}$$

for an $\omega_0$ for which $F$ has decayed to one-half of its peak value. This quantity equals unity for all profiles that satisfy Eq. (19). For the $\lambda L = 01$ and 23 components in the fundamental band, however, this quantity is always greater than unity and rises rapidly with temperature, as Fig. 7 shows. In other words, at the half intensity point the condition, Eq. (19), is violated by 10% and 22% at low temperatures for the quadrupole- and overlap-induced components, respectively. (The $\lambda L = 45$ and 21 differ by similar amounts.) At the higher temperatures, much more substantial violations amounting to 50% or more are observed which can hardly be ignored.

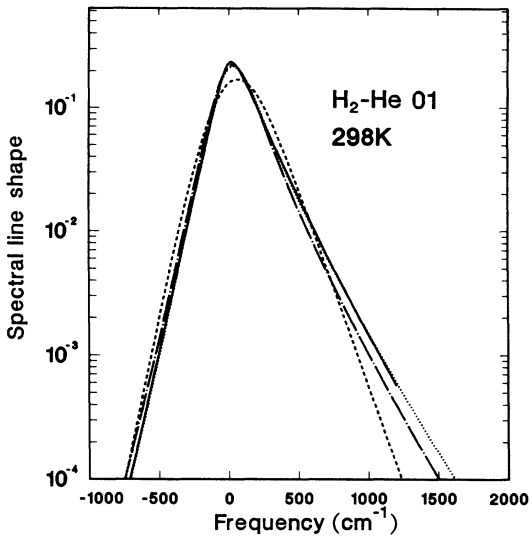


FIG. 6. Spectral profile of $H_2$-He complexes, arising from quadrupolar induction in the fundamental band of hydrogen at 298 K. Shown are the exact profiles (solid line), the $v$-dependent model representing the exact profile (dotted line), and the familiar BC profile which satisfies Eq. (19) instead of Eq. (20) (dashed line). For comparison, we also show the BC profile obtained from $v$-independent moment calculations (dash-dot line).

## V. CONCLUSION

In general terms as well as by the example of the fundamental band of $H_2$-He pairs, we have demonstrated that commonly used model profiles exhibit a symmetry which is not consistent with that of RVCIA profiles. We observe a close representation of the exact quantum profiles of RVCIA spectra if model functions of the proper symmetry are constructed according to simple procedures given. The modifications of symmetry described are of a special significance at high temperatures (stellar

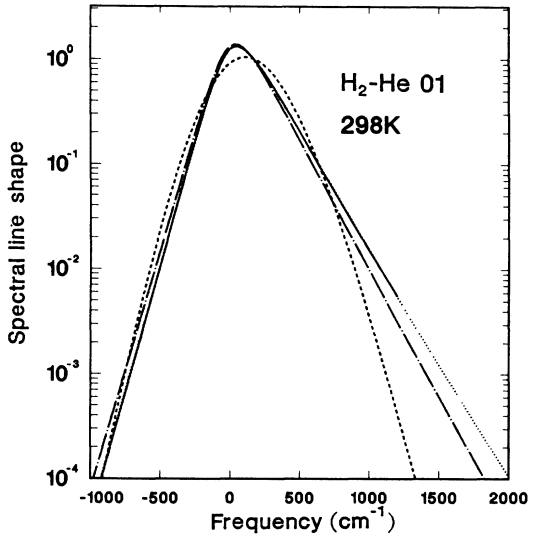


FIG. 5. Spectral profile of $H_2$-He complexes, arising from isotropic overlap induction in the fundamental band of hydrogen at 298 K. Shown are the exact profile (solid line), the $v$-dependent model representing the exact profile (dotted line, nearly indistinguishable from the exact profile), and the familiar $K_0$ profile which satisfies Eq. (19) instead of Eq. (20) (dashed line). For comparison, we show the $K_0$ profile obtained from $v$-independent moment calculations (dash-dot line).

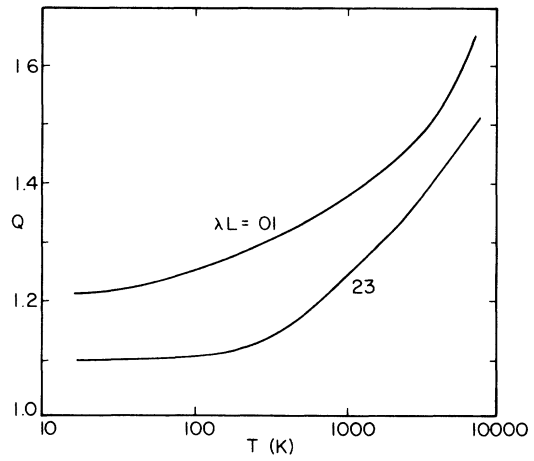


FIG. 7. The parameter $Q$ [Eq. (46)] as a function of temperature which shows the degree of validity of the commonly used detailed balance equation, Eq. (19), for the fundamental band of $H_2$-He. If Eq. (19) were valid, $Q$ should equal unit at all temperatures. The test is made at a frequency $\omega_0$ where the intensity of the "blue" wing has fallen off to one-half of the peak intensity.

atmospheres) in all vibrational CIA bands, especially for the overtone and hot bands. For $H_2$-$H_2$ pairs, indeed for almost any complex involving at least one molecule, similar results are to be expected, but due to the lack of an interaction potential for hydrogen pairs that accurately accounts for the vibrational dependences, no such computations are shown at this time. The results of this work are significant for the modeling of planetary and stellar atmospheres containing molecular hydrogen, and for the analyses of RVCIA spectra in general.

## ACKNOWLEDGMENT

The hospitality and friendly support of Dr. Jeffrey Linsky is gratefully acknowledged. The work of two of us (A.B. and L.F.) was supported by the National Science Foundation, Grant No. AST-8613085. Affiliation of M.M.: Dipartimento di Fisica dell'Università di Firenze et Unità di Firenze, Gruppo Nazionale di Struttura della Materia, and Centro Interuniversitario di Struttura della Materia (GNSM-CISM).

[1]H. L. Welsh, in *Spectroscopy,* Vol. III of *MTP International Review of Science—Physical Chemistry,* edited by A. D. Buckingham and D. A. Ramsay (Butterworths, London, 1972), Series 1, p. 33.
[2]J. van Kranendonk, Physica **73**, 156 (1974).
[3]J. D. Poll and J. van Kranendonk, Can. J. Phys. **39**, 189 (1961).
[4]A. D. Buckingham, Colloq. Int. C.N.R.S. **77**, 57 (1959).
[5]K. L. C. Hunt, in *Phenomena Induced by Intermolecular Interactions,* edited by G. Birnbaum (Plenum, New York, 1985), p. 1.
[6]J. van Kranendonk and R. B. Bird, Physica **17**, 953 (1951).
[7]J. van Kranendonk and R. B. Bird, Physica **17**, 968 (1951).
[8]R. W. Patch, J. Quant. Spectrosc. Radiat. Transfer **11**, 1331 (1971).
[9]R. W. Patch, J. Quant. Spectrosc. Radiat. Transfer **14**, 101 (1974).
[10]P. E. S. Wormer and G. van Dijk, J. Chem. Phys. **70**, 5695 (1979).
[11]W. Meyer, in *Phenomena Induced by Intermolecular Interactions,* edited by G. Birnbaum (Plenum, New York, 1985), p. 29.
[12]W. Meyer and L. Frommhold, Phys. Rev. A **34**, 2771 (1986).
[13]W. Meyer, L. Frommhold, and G. Birnbaum (unpublished).
[14]G. Birnbaum, S. Chu, A. Dalgarno, L. Frommhold, and E. L. Wright, Phys. Rev. A **29**, 595 (1984).
[15]J. Borysow and L. Frommhold, in *Phenomena Induced by Intermolecular Interactions,* edited by G. Birnbaum (Plenum, New York, 1985), p. 67.
[16]W. Meyer and L. Frommhold, Phys. Rev. A **34**, 2936 (1986).
[17]L. Frommhold and W. Meyer, Phys. Rev. A **35**, 632 (1987).
[18]R. H. Tipping, in *Phenomena Induced by Intermolecular Interactions,* edited by G. Birnbaum (Plenum, New York, 1985), p. 727.
[19]G. B. Field, W. B. Somerville, and K. Dressler, Ann. Rev. Astron. Astrophysics **4**, 207 (1966).
[20]L. M. Trafton, Astrophys. J. **146**, 558 (1966).
[21]L. M. Trafton, Astrophys. J. **179**, 971 (1973).
[22]J. L. Linsky, Astrophys. J. **156**, 989 (1969).
[23]R. W. Patch, J. Quant. Spectrosc. Radiat. Transfer **11**, 1311 (1971).
[24]R. W. Patch, J. Quant. Spectrosc. Radiat. Transfer **14**, 49 (1974).
[25]H. L. Shipman, Astrophys. J. **213**, 138 (1977).
[26]J. Mould and J. Liebert, Astrophys. J. **266**, L29 (1978).
[27]F. Palla, in *Molecular Astrophysics—State of the Art and Future Directions,* edited by G. H. F. Diercksen, W. F. Huebner, and P. W. Langhoff (Reidel, Dordrecht, 1985), p. 687.
[28]S. W. Stahler, F. Palla, and E. E. Salpeter, Astrophys. J. **302**, 590 (1986).
[29]J. Schäfer and W. Meyer, in *Electronic and Atomic Collisions,* edited by J. Eichler, I. V. Hertel, and N. Stolterfoht (North-Holland, Amsterdam, 1984), p. 524.
[30]J. Borysow, L. Trafton, L. Frommhold, G. Birnbaum, Astrophys. J. **296**, 644 (1985).
[31]J. Borysow, L. Frommhold, and G. Birnbaum, Astrophys. J. **326**, 509 (1988).
[32](a) M. Moraldi, J. Borysow, and L. Frommhold, Phys. Rev. A **36**, 4700 (1987); (b) A. Borysow and L. Frommhold (unpublished).
[33]G. Birnbaum and E. R. Cohen, Can. J. Phys. **54**, 593 (1976).
[34]G. Birnbaum, B. Guillot, and S. Bratos, Adv. Chem. Phys. **51**, 49 (1982).
[35]S. P. Reddy, in *Phenomena Induced by Intermolecular Interactions,* edited by G. Birnbaum (Plenum, New York, 1985), p. 129.
[36]L. Frommhold, in *Advances in Chemical Physics,* edited by I. Prigogine and S. Rice (Wiley, New York, 1981), Vol. 46, p. 1; see also an update in Can. J. Phys. **59**, 1459 (1981).
[37]J. Borysow and L. Frommhold, in *Phenomena Induced by Intermolecular Interactions,* edited by G. Birnbaum (Plenum, New York, 1985), p. 67.
[38]J. L. Hunt and J. D. Poll, Can. J. Phys. **56**, 950 (1978).
[39]J. D. Poll and J. L. Hunt, Can. J. Phys. **54**, 461 (1976).
[40]W. Meyer, P. C. Hariharan, and W. Kutzelnigg, J. Chem. Phys. **73**, 1880 (1980).
[41]A. Borysow, M. Moraldi, and L. Frommhold, J. Quant. Spectrosc. Radiat. Transfer **31**, 235 (1984).
[42]M. Moraldi, Chem. Phys. **78**, 243 (1983).
[43]M. Moraldi, A. Borysow, and L. Frommhold, Chem. Phys. **86**, 339 (1984).
[44]R. W. Hartye, C. G. Gray, J. D. Poll, and M. S. Miller, Mol. Phys. **29**, 825 (1975).
[45]J. Borysow, M. Moraldi, and L. Frommhold, Mol. Phys. **56**, 913 (1985).
[46]A. Borysow and L. Frommhold, Astrophys. J. **318**, 940 (1987).